Monthly Notices of the ROYAL ASTRONOMICAL SOCIETY

MNRAS **467,** 412–427 (2017)
Advance Access publication 2017 January 12

doi:10.1093/mnras/stx079

Globular clusters with *Gaia*

E. Pancino,[1,2★] M. Bellazzini,[3] G. Giuffrida[4,2] and S. Marinoni[4,2]

[1]*INAF-Osservatorio Astrofisico di Arcetri, Largo Enrico Fermi 5, I-50125 Firenze, Italy*
[2]*ASI Science Data Center, Via del Politecnico SNC, I-00133 Rome, Italy*
[3]*INAF-Osservatorio Astronomico di Bologna, Via Ranzani 1, I-40127 Bologna, Italy*
[4]*INAF-Osservatorio Astronomico di Roma, Via di Frascati 33, I-00044 Monteporzio Catone, Italy*

Accepted 2017 January 10. Received 2017 January 9; in original form 2016 November 17

ABSTRACT

The treatment of crowded fields in *Gaia* data will only be a reality in a few years from now. In particular, for globular clusters, only the end-of-mission data (public in 2022–2023) will have the necessary full crowding treatment and will reach sufficient quality for the faintest stars. As a consequence, the work on the deblending and decontamination pipelines is still ongoing. We describe the present status of the pipelines for different *Gaia* instruments, and we model the end-of-mission crowding errors on the basis of available information. We then apply the nominal post-launch *Gaia* performances, appropriately worsened by the estimated crowding errors, to a set of 18 simulated globular clusters with different concentration, distance and field contamination. We conclude that there will be 10^3–10^4 stars with astrometric performances virtually untouched by crowding (contaminated by <1 mmag) in the majority of clusters. The most limiting factor will be field crowding, not cluster crowding: the most contaminated clusters will only contain 10–100 clean stars. We also conclude that (i) the systemic proper motions and parallaxes will be determined to 1 per cent or better up to $\simeq$15 kpc, and the nearby clusters will have radial velocities to a few km s^{-1}; (ii) internal kinematics will be of unprecedented quality, cluster masses will be determined to $\simeq$10 per cent up to 15 kpc and beyond, and it will be possible to identify differences of a few km s^{-1} or less in the kinematics (if any) of cluster sub-populations up to 10 kpc and beyond; (iii) the brightest stars ($V \simeq 17$ mag) will have space-quality, wide-field photometry (mmag errors), and all *Gaia* photometry will have 1–3 per cent errors on the absolute photometric calibration.

Key words: astrometry – parallaxes – globular clusters: general.

1 INTRODUCTION

The ESA[1] (European Space Agency) space mission *Gaia*[2] (Perryman et al. 2001; Mignard 2005; Gaia Collaboration 2016a,b) is the successor of *Hipparcos* (Perryman et al. 1997), with the goal of providing astrometry for billions of point-like sources across the whole sky, with an error of 24 μas-level for stars of $G \simeq 15$ mag. *Gaia* will also provide broad-band magnitudes and colours for all sources, down to the *Gaia* white-light magnitude of $G = 20.7$ mag ($V \simeq 21$ mag). Low-dispersion spectra will also be obtained in two broad-bands with the red and blue spectrophotometers (BP and RP). Finally, *Gaia* will produce spectra in the calcium triplet region with the RVS (the radial velocity spectrometer) down to $G \simeq 17$ mag, from which radial velocities (RVs). Object classification and parametrization will be possible for all sources. *Gaia* was launched in 2013 December (de Bruijne, Rygl & Antoja 2014), and the first data release was in 2016 September (Gaia Collaboration 2016b), containing positions and white-light magnitudes for the best behaved stars, and additional information like parallaxes and proper motions for $\simeq$2 million stars observed previously with *Tycho-2* (Høg et al. 2000; Michalik, Lindegren & Hobbs 2015; Lindegren et al. 2016).

Gaia will observe not only stars, but also tens of thousands of quasars, unresolved galaxies, Solar system objects, many transient and variable objects like supernovae, and finally the interstellar medium (Altavilla et al. 2012; Ducourant et al. 2014; Eyer et al. 2014; de Bruijne et al. 2015; Proft & Wambsganss 2015; Zwitter & Kos 2015; Bachchan, Hobbs & Lindegren 2016; Tanga et al. 2016). *Gaia* will also pose a challenge because of its data amount and complexity, pushing the astrophysical community farther into the path of big data and data mining (Gaia Collaboration 2016a).

Gaia is limited in dense stellar fields, owing to the onboard and downstream telemetry bandwidth. For spectroscopy, an additional

★E-mail: pancino@arcetri.inaf.it
[1] A list of the acronyms used in this paper (Table A1) can be found in Appendix A.
[2] http://www.cosmos.esa.int/web/gaia

limitation is provided by the large physical size of the dispersed images and spectra on the focal plane. This has particular relevance for studies of the Galactic plane, the bulge and globular clusters (hereafter, GCs). In the first few *Gaia* data releases, disturbed sources like binaries, multiple stars and stars in crowded fields will likely not be part of the released material (Gaia Collaboration 2016b). In any case, the inclusion of a sufficient sample of stars at the main-sequence turn-off point or fainter – with good-quality measurements – is very important for GC research. Therefore, only the latest few *Gaia* releases (2020–2023) are expected to provide a significant breakthrough in GC research. To prepare the work, we explore in this paper the expected behaviour of *Gaia* data in several simulated Galactic GCs, adopting the official post-launch *Gaia* science performances and some simplified recipes to describe additional deblending error components, based on the *Gaia* deblending pipelines. A very preliminary – and now outdated – version of this work was presented by Pancino, Bellazzini & Marinoni (2013).

This paper is organized as follows. In Section 2, we describe the current status of crowding treatment in *Gaia*; in Section 3, we present our crowding errors modelling; in Section 4, we describe our simulated clusters and the computation of *Gaia* observed quantities and final errors; in Section 5, we explore the simulations and show the potential of *Gaia* data for GC studies; in Section 6, we summarize the main results and draw our conclusions.

2 CROWDING IN *GAIA* DATA

As mentioned in the previous section, *Gaia* is a complex space mission, with two different telescopes projecting their light on a large common focal plane, captured by 106 different CCDs (charge-coupled devices), and passing through different instruments. *Gaia* scans the whole sky by precessing its spin axis, and describing great circles on the sky that slowly drift with its precession. Each region is scanned from a minimum of $\simeq$40 times, to a maximum of $\simeq$250 times, with an average number of $\simeq$70 passages for the AF, BP and RP, and $\simeq$40 passages for RVS. All the CCDs in the focal plane are read in TDI (time-delayed integration) mode to closely follow *Gaia*'s movement across the sky. On the focal plane, stars 'move' along the scanning direction, encountering different instruments:

(i) The first two columns of the CCD array are called Sky Mappers (SM), and they are used for the onboard detection of point-like sources; each of the SM columns sees only light from one of the two telescopes.

(ii) The AF (astrometric field) provides astrometry and photometry of point-like sources in the G band, a white-light passband defined by the telescope and instrument transmission and by the CCD quantum efficiency (Fig. 1).

(iii) The BP and RP provide low-resolution spectra ($R = \lambda/\delta\lambda =$ 20–100) in the ranges shown in Fig. 1, and the integrated $G_{\rm BP}$ and $G_{\rm RP}$ magnitudes; the spectra are necessary for the chromaticity displacement correction in astrometric measurements.

(iv) The RVS provides $R \simeq 11\,700$ spectra in the calcium triplet region, for stars down to $G \simeq 17$ mag, depending on the object.

To save telemetry bandwidth, given the enormous amount of data produced daily by *Gaia*, observations in each instrument are only transmitted for pixels contained in rectangular windows, that follow the detected point-like objects along the focal plane. For the faint stars, data in the allocated windows are binned in the AC direction by the onboard processing software. The adopted window sizes and relevant quantities for our treatment of crowding are listed in Table 1. More information can be found in the *Gaia* mission paper (Gaia Collaboration 2016a).

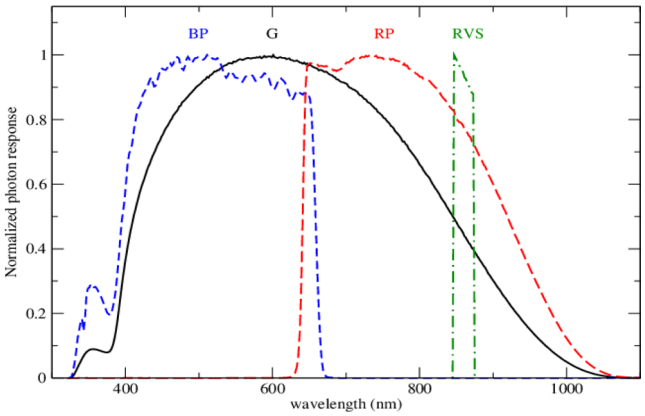

Figure 1. The *Gaia* nominal passbands for the astrometric field (G band), the blue and red spectrophotometers (BP and RP) and the radial velocity spectrometer (RVS). Figure courtesy of C. Jordi.

Table 1. Adopted *Gaia* relevant quantities. We note that the AF window sizes are relevant for the astrometry; the BP/RP sizes for the photometry, chromaticity correction, and object classification and parametrization; the RVS window sizes are relevant for RV, object parametrization and abundance analysis.

Size (arcsec)	Size (pix)	Description
0.176 789	1 (AC)	Across scan (AC) pixel size
0.058 933	1 (AL)	Along scan (AL) pixel size
0.176 789	3 (AL)	*Gaia* PSF
2.121 468	12 (AC)	AC window size (AF, BP and RP)
0.070 720	12 (AL)	AL window size (AF)[a]
1.767 890	10 (AC)	AC window size (RVS)
3.535 980	60 (AL)	AL window size (BP and RP)
74.785 977	1269 (AL)	AL window size (RVS)

[a]In some CCD columns in AF, as well as in the SM CCD columns, the windows are longer to allow for background measurements around the sources. The longer wings of these windows can in principle be used also to check the source profile behaviour outside normal window limits.

2.1 *Gaia* deblending and decontamination pipelines

Crowding treatment ideally requires a preliminary evaluation of the crowding conditions of each source and transit, based on knowledge of the *scene*, i.e. the distribution and characteristics of all the neighbouring sources, as collected before the current observation. Different pipelines are employed for different instruments and to treat different cases. Below we describe the current status of the ones that are relevant for this study.

2.1.1 AF deblending

Stars closer than the *Gaia* PSF width (which is assumed here[3] to be 0.177 arcsec, see also Table 1) can be recognized as blends already in the astrometric processing of AF data. These blends can be detected, for example, from the high errors in the centroid

[3] The value we adopted is a conservative estimate. The *Gaia effective* PSF varies across the field of view and has a median value of 0.103 arcsec (Fabricius et al. 2016).

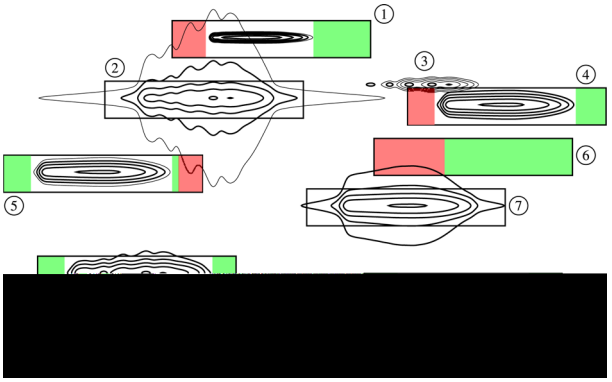

Figure 2. An illustration of the crowding effects on BP and RP dispersed images, with their assigned windows (black rectangles). Different cases are represented, some going beyond the scope of this paper. Stars are represented by their surface density profiles (solid contours), with the outmost contours at the background level. The brightest star ($G = 15$ mag) is in window (2), while the faintest one ($G = 20$ mag) is in window (1). Stars fainter than the *Gaia* magnitude limit ($G = 20.7$ mag) are assigned no window, like for star (3). The coloured portions of the windows are the background samples, in green when they are free from contamination, and in red when they are contaminated and cannot be used. When stars are too close, they can be assigned to the same widow or two (or more) truncated windows, like in cases (9), (10) and (11). There are also empty windows (virtual objects) like in case (6). Figure courtesy of A. Brown.

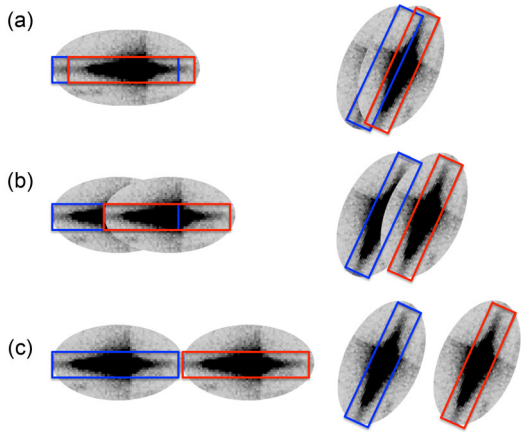

Figure 3. Simplified description of transits in BP/RP. In case (a), two stars are closer than half the AC window size, and no matter the orientation of the satellite, they will always be assigned the same window (or truncated windows). In case (b), two stars have a distance that is in between the AC and AL half window sizes, and depending on the orientation, they are sometimes assigned the same window (or truncated window), sometimes different windows. Depending on their brightness, they can still contaminate each other's window. In case (c), the stars are farther apart than the AL window size, and they are always assigned two different windows but, if one of the two stars is very bright, it can still contaminate the other significantly.

determination and its wobbling from one transit to another, or by photometric variability, RV variability, or in general because the fits of the PSF or LSF to the data show large residuals or require more than one component.

Assessing whether a star is isolated or has detected or suspected companions is a crucial task. Multiple or blended objects are redirected to the NSS (non-single stars) pipeline where an attempt to model them as binary systems is carried out (Pourbaix 2011; Gaia Collaboration 2016a). If none of the available binary models or configurations produces a good fit to the data, then a stochastic model is employed to derive preliminary parameters of the secondary (or tertiary and so on) source. Therefore we can assume that – considering also the small *Gaia* PSF – the vast majority of NSS will be known.

Stars that are further apart than the tiny *Gaia* PSF are easily deblended by the PSF fitting algorithms, with results much more similar to *HST* (*Hubble Space Telescope*) than to typical ground-based telescopes. This is the main reason why – as we will see in the following – astrometric measurement uncertainties (and G magnitudes) are in general less affected by crowding, unlike BP/RP and RVS measurements.

2.1.2 BP and RP deblending and decontamination pipelines

BP and RP transits of sources that are not isolated will be called here either *blended* or *contaminated*. The idea is that when the sources are so close that they occupy the same window or interfering windows in the vast majority of the transits (*blends*, with $D < 2.12$ arcsec), they will require a different treatment than objects that will often be assigned well-separated windows, or transits that are just altered by the flux of a bright source that is well outside of the window (*contaminants*, with $D < 3.54$ arcsec). This is illustrated in Fig. 2, where different cases are shown together with the background evaluation regions, and in Fig. 3, showing how the differing orientation and AL projected distance between sources affects window assignment.

For blended sources, there are different pipelines that can be used in different phases of the mission. Blind pipelines (without knowledge of the scene) can be applied in the initial phases, when the history of each source in different instruments has not built up to a sufficient level. The two (or more) blended sources can be roughly modelled without a priori knowledge of their exact positions, astrophysical parameters and fluxes, just by modelling them with two overlapping spectral energy distributions. This approach was successfully applied to *Gaia* commissioning data[4] of bright stars, recovering the vast majority of the Ticho-2 binary and double stars. Once a few transits are accumulated, they can be better disentangled if they are modelled simultaneously (*per source* rather than *per transit*), even if there is still not enough information on the scene, improving the quality of the reconstruction. Finally, once the scene is well characterized and the history of the source is well developed, other parameters of the modelling like the spectral type, the projected distance of the sources along scan and the relative fluxes, can be used to further improve the involved sources reconstruction.

For contaminated sources, it is necessary to know well the flux of the contaminating sources around, thus knowledge of the scene is necessary. Each known source is modelled to reconstruct the flux even at large distances from the window (especially for bright stars). The amount of reconstructed contaminating flux from neighbouring sources is computed in each pixel of the contaminated source window, and subtracted. For all these reasons, decontamination will have to be performed contextually with the scene reconstruction and crowding evaluation.

2.1.3 RVS deblending and decontamination pipelines

The deblending philosophy adopted by RVS is slightly different from the one adopted in AF, or BP and RP. The deblending pipelines are being adapted and rewritten to mitigate the stray light issues

[4] http://www.cosmos.esa.int/web/gaia/iow_20150226

(iv) The distances of GCs will be obtained with errors of $\simeq$1 per cent, and for GCs heavily contaminated by field stars to a few per cent. The impact on the determinations of stellar masses and ages will be significant. It is expected that GC absolute ages with errors below 10 per cent will be obtained. Also, better estimates of surface gravities for GC stars with known distances will remove one of the major uncertainty sources from abundance determinations with high-resolution spectroscopy.

(v) While it is difficult to simulate the exact completeness level of *Gaia* in GCs, we have shown that the astrometric performances are still exceptional in the central arcminute of the simulated GCs: most of the stars have errors around a few 100 μas or μas yr^{-1}.

(vi) The BP/RP photometry and the RVS spectra, on the other hand, have larger AL sizes and therefore suffer more from crowding effects. The most important factor for these instruments is crowding by field stars, especially in the most extreme cases like the bulge field, which acts at all distances from the GC centre and combines with the crowding effects from GC stars in the central regions.

The imminent decision of whether to extend the *Gaia* mission lifetime will certainly have a beneficial impact on all the above measurements. However, the simulations presented here are already pessimistic and the pipelines are expected to evolve significantly in the next few years. Therefore, we conclude that *Gaia* measurements will revolutionize our knowledge of GCs.

ACKNOWLEDGEMENTS

We warmly thank A. Brown, M. Castellani, A. Di Cecco, F. De Luise, D. Harrison, H. E. Huckle, K. Janssen, C. Jordi, P. M. Marrese, D. Pourbaix, L. Pulone and G. Seabroke, for providing useful information about *Gaia* BP, RP and RVS deblending and decontamination, and for enlightening discussions about *Gaia* and crowded fields treatment in general. This work used simulated data provided by the Simulation Unit (CU2) of the Gaia Data Processing and Analysis Consortium (DPAC), run with GIBIS at CNES (Centre national d'études spatiales). This research has made use of the R programming language (https://www.r-project.org/) and more specifically of its 'DATA.TABLE' package, for the treatment of very large data sets. Some of the figures were prepared with TOPCAT (Taylor 2005).

REFERENCES

Allende Prieto C., 2008, Gaia Technical Note number GAIA-C6-SP-MSSL-CAP-003
Altavilla G., Botticella M. T., Cappellaro E., Turatto M., 2012, Ap&SS, 341, 163
Altavilla G. et al., 2015, Astron. Nachr., 336, 515
An J., Evans N. W., Deason A. J., 2012, MNRAS, 420, 2562
Babusiaux C., 2005, in Turon C., O'Flaherty K. S., Perryman M. A. C., eds, ESA SP-576: The Three-Dimensional Universe with Gaia. ESA, Noordwijk, p. 417
Bachchan R. K., Hobbs D., Lindegren L., 2016, A&A, 589, A71
Bailer-Jones C. A. L., 2015, PASP, 127, 994
Bellazzini M., Bragaglia A., Carretta E., Gratton R. G., Lucatello S., Catanzaro G., Leone F., 2012, A&A, 538, A18
Bellini A. et al., 2014, ApJ, 797, 115
Bohlin R. C., Gilliland R. L., 2004, AJ, 127, 3508
Brodie J. P., Strader J., 2006, ARA&A, 44, 193
de Bruijne J. H. J., Rygl K. L. J., Antoja T., 2014, EAS Publ. Ser. Vol. 67, Gaia Astrometric Science Performance – Post-Launch Predictions. EDP Sciences, Les Ullis, p. 23
de Bruijne J. H. J., Allen M., Azaz S., Krone-Martins A., Prod'homme T., Hestroffer D., 2015, A&A, 576, A74
Dinescu D. I., van Altena W. F., Girard T. M., López C. E., 1999, AJ, 117, 277
Ducourant C., Krone-Martins A., Galluccio L., Teixeira R., 2014, in Ballet J., Martins F., Bournaud F., Monier R., Reylé C., eds, Proc. Ann. French Soc. Astron. Astrophys., Gaia and the Extragalactic. p. 421
Eyer L. et al., 2014, in Walton N. A., Figueras F., Balaguer-Núñez L., Soubiran C., eds, EAS Publ. Ser. Vol. 67, The Milky Way Unravelled by Gaia: GREAT Science from the Gaia Data Releases. p. 75
Fabricius C. et al., 2016, A&A, 595, A3
Feuillet D. K., Bovy J., Holtzman J., Girardi L., MacDonald N., Majewski S. R., Nidever D. L., 2016, ApJ, 817, 40
Gaia Collaboration, 2016a, A&A, 595, A1
Gaia Collaboration, 2016b, A&A, 595, A2
Gratton R. G., Fusi Pecci F., Carretta E., Clementini G., Corsi C. E., Lattanzi M., 1997, ApJ, 491, 749
Gratton R., Sneden C., Carretta E., 2004, ARA&A, 42, 385
Harris W. E., 1996, AJ, 112, 1487
Harrison D. L., 2011, Exp. Astron., 31, 157
Hendra Gunadi A., 2011, Master thesis, Australian National University
Hénault-Brunet V., Gieles M., Agertz O., Read J. I., 2015, MNRAS, 450, 1164
Hurley J. R., Pols O. R., Tout C. A., 2000, MNRAS, 315, 543
Høg E. et al., 2000, A&A, 355, L27
Jordi C. et al., 2006, MNRAS, 367, 290
Jordi C. et al., 2010, A&A, 523, A48
King I. R., 1966, AJ, 71, 64
Kordopatis G., Recio-Blanco A., de Laverny P., Bijaoui A., Hill V., Gilmore G., Wyse R. F. G., Ordenovic C., 2012, EPJ Web Conf., 19, 09010
Kordopatis G. et al., 2013, AJ, 146, 134
Kraft R. P., 1994, PASP, 106, 553
Kroupa P., 2001, MNRAS, 322, 231
Küpper A. H. W., Maschberger T., Kroupa P., Baumgardt H., 2011, MNRAS, 417, 2300
Lindegren L. et al., 2016, A&A, 595, A4
Marinoni S. et al., 2016, MNRAS, 462, 3616
Martin N. F., Ibata R. A., Chapman S. C., Irwin M., Lewis G. F., 2007, MNRAS, 380, 281
Michalik D., Lindegren L., Hobbs D., 2015, A&A, 574, A115
Mignard F., 2005, in Seidelmann P. K., Monet A. K. B., eds, ASP Conf. Ser. Vol. 338, Astrometry in the Age of the Next Generation of Large Telescopes. Astron. Soc. Pac., San Francisco, p. 15
Mora A. et al., 2016, in MacEwen H. A., Fazio G. G., Lystrupeds M., Batalha N., Siegler N., Tong E. C., eds, Proc. SPIE Conf. Ser. Vol. 9904, Space Telescopes and Instrumentation 2016: Optical, Infrared, and Millimeter Wave. SPIE, Bellingham, p. 99042D
Pancino E. et al., 2012, MNRAS, 426, 1767
Pancino E., Bellazzini M., Marinoni S., 2013, Mem. Soc. Astron. Ital., 84, 83
Paust N. E. Q. et al., 2010, AJ, 139, 476
Peñarrubia J., Koposov S. E., Walker M. G., 2012, ApJ, 760, 2
Perryman M. A. C. et al., 1997, A&A, 323, 49
Perryman M. A. C. et al., 2001, A&A, 369, 339
Piersimoni A., De Luise F., Busso G., 2011, Gaia Technical Note number GAIA-C5-TN-OATE-AP-001
Pourbaix D., 2011, in Docobo J. A., Tamazian V. S., Balega Y. Y., eds, AIP Conf. Proc. Vol. 1346, International Workshop on Double and Multiple Stars: Dynamics, Physics, and Instrumentation. Am. Inst. Phys., New York, p. 122
Price-Whelan A. M., Hogg D. W., Johnston K. V., Hendel D., 2014, ApJ, 794, 4
Proft S., Wambsganss J., 2015, A&A, 574, A46
Pryor C., Meylan G., 1993, in Djorgovski S. G., Meylan G., eds, Proc. ASP Conf. Ser. Vol. 50, Structure and Dynamics of Globular Clusters. Astron. Soc. Pac., San Francisco, p. 357
Puspitarini L. et al., 2015, A&A, 573, A35
Robin A. C., Reylé C., Derrière S., Picaud S., 2003, A&A, 409, 523
Seabroke G. et al., 2016, in Bragaglia A., Arnaboldi M., Rejkuba M., Romano D., eds, Proc. IAU Symp. 317, The General Assembly of Galaxy

Halos: Structure, Origin and Evolution. Cambridge Univ. Press, Cambridge, p. 346
Sollima A., Baumgardt H., Zocchi A., Balbinot E., Gieles M., Hénault-Brunet V., Varri A. L., 2015, MNRAS, 451, 2185
Sollima A. et al., 2016, MNRAS, 462, 1937
Tanga P. et al., 2016, Planet. Space Sci., 123, 87
Taylor M. B., 2005, in Shopbell P., Britton M., Ebert R., eds, ASP Conf. Ser. Vol. 347, Astronomical Data Analysis Software and Systems XIV. Astron. Soc. Pac., San Francisco, p. 29
Walker M. G., Mateo M., Olszewski E. W., Bernstein R., Wang X., Woodroofe M., 2006, AJ, 131, 2114
Zwitter T., Kos J., 2015, Mem. Soc. Astron. Ital., 86, 541

SUPPORTING INFORMATION

Supplementary data are available at *MNRAS* online.

Table 3. Column-by-column description of the final simulated stars.

Please note: Oxford University Press is not responsible for the content or functionality of any supporting materials supplied by the authors. Any queries (other than missing material) should be directed to the corresponding author for the article.

APPENDIX A: LIST OF ACRONYMS

Table A1 lists all the acronyms used.

Table A1. List of acronyms used in this paper.

Acronym	Description
AC	ACross scan
AF	Astrometric field
AL	ALong scan
BP	Blue spectro-Photometer
CCD	Charge-coupled device
CDS	Centre de Données astronomiques de Strasbourg
CMD	Colour–magnitude diagram
CNES	Centre National d'Études Spatiales
DPAC	Data Processing and Analysis Consortium
ESA	European Space Agency
FWHM	Full width at half-maximum
GIBIS	Gaia Instrument and Basic Image Simulator
GC	Globular cluster
HB	Horizontal branch
HST	*Hubble Space Telescope*
IMF	Initial mass function
LSF	Line spread function
MLE	Maximum likelihood estimator
MW	Milky Way
NSS	Non-single stars
PSF	Point spread function
RAVE	RAdial Velocity Experiment
RP	Red spectro-Photometer
RV	Radial velocity
RVS	Radial velocity spectrometer
SEA	Source Environment Analysis
SM	Sky Mapper
TDI	Time-delayed integration

Table A1 – *continued*

This paper has been typeset from a TEX/LATEX file prepared by the author.